Environ Monit Assess (2017) 189: 6
DOI 10.1007/s10661-016-5659-7

The relationship between aerosol particles chemical composition and optical properties to identify the biomass burning contribution to fine particles concentration: a case study for São Paulo city, Brazil

Regina Maura de Miranda · Fabio Lopes · Nilton Évora do Rosário · Marcia Akemi Yamasoe · Eduardo Landulfo · Maria de Fatima Andrade

Received: 23 March 2016 / Accepted: 21 October 2016 / Published online: 5 December 2016

Abstract The air quality in the Metropolitan Area of São Paulo (MASP) is primarily determined by the local pollution source contribution, mainly the vehicular fleet, but there is a concern about the role of remote sources to the fine mode particles ($PM_{2.5}$) concentration and composition. One of the most important remote sources of atmospheric aerosol is the biomass burning emissions from São Paulo state's inland and from the central and north portions of Brazil. This study presents a synergy of different measurements of atmospheric aerosol chemistry and optical properties in the MASP in order to show how they can be used as a tool to identify particles from local and remote sources. For the clear identification of the local and remote source contribution, aerosol properties measurements at surface level were combined with vertical profiles information. Over 15 days in the austral winter of 2012, particulate matter (PM) was collected using a cascade impactor and a Partisol sampler in São Paulo City. Mass concentrations were determined by gravimetry, black carbon concentrations by reflectance, and trace element concentrations by X-ray fluorescence. Aerosol optical properties were studied using a multifilter rotating shadowband radiometer (MFRSR), a Lidar system and satellite data. Optical properties, concentrations, size distributions, and elemental composition of atmospheric particles were strongly related and varied according to meteorological conditions. During the sampling period, PM mean mass concentrations were 17.4 ± 10.1 and 15.3 ± 6.9 μg/m^3 for the fine and coarse fractions, respectively. The mean aerosol optical depths at 415 nm and Ångström exponent (AE) over the whole period were 0.29 ± 0.14 and 1.35 ± 0.11, respectively. Lidar ratios reached values of 75 sr. The analyses of the impacts of an event of biomass burning smoke transport to the São Paulo city revealed significant changing on local aerosol concentrations and optical parameters. The identification of the source contributions, local and remote, to the fine particles in MASP can be more precisely achieved when particle size composition and distribution, vertical profile of aerosols, and air mass trajectories are analyzed in combination.

Keywords Urban aerosols · Biomass burning · Chemical composition · Optical properties

R. M. de Miranda (✉)
School of Arts, Sciences, and Humanities, University of São Paulo, Rua Arlindo Béttio1000, Ermelino Matarazzo, São Paulo, SP 03828-000, Brazil
e-mail: remaura@usp.br

F. Lopes · M. A. Yamasoe · M. de Fatima Andrade
Instituto de Astronomia, Geofísica e Ciências Atmosféricas, Departamento de Ciências Atmosféricas, Universidade de São Paulo, Rua do Matão 1226, São Paulo, SP 05508-090, Brazil

N. É. do Rosário
Environmental Sciences Department, Federal University of São Paulo, Rua Prof. Artur Riedel 275, Jd. Eldorado, Diadema, SP 09972-270, Brazil

E. Landulfo
Nuclear and Energy Research Institute, IPEN-CNEN/SP, Av Lineu Prestes 2242, São Paulo, SP 05508-000, Brazil

Introduction

Atmospheric aerosol particles are naturally expected to have different chemical compositions and physical properties (size and shape) since they come from distinct natural and anthropogenic sources. However, meteorological conditions, sources, and sinks of particles and geographical distribution also play a major role on the spatial and temporal variability of aerosol particles' chemical and microphysical properties throughout the atmosphere. Since the climatic effects of atmospheric aerosol particles strongly rely on their chemical and physical properties, the characterization and the understanding of spatial and temporal variation of particle properties in the atmosphere are important and a matter of ongoing research. Particulate matter (PM) suspended in the atmosphere can influence the amount of solar radiation that reaches the Earth's surface through scattering and absorption processes (Seinfeld and Pandis 2006). The resulting redistribution of shortwave radiation into the atmosphere can cause the heating or cooling of the atmosphere, depending on the physicochemical and optical properties of the particles (IPCC 2013). A second radiative effect from aerosols is related to their ability to modify the optical properties, amount, and lifetime of clouds, which is known as aerosol indirect effect (Liu et al. 2014). Metropolitan areas are significant sources of aerosols which are released into the regional atmosphere. At the same time, these regions are often affected by particulate matter transported from distant areas. Therefore, improving the current knowledge regarding the sources, microphysical and optical properties of urban aerosols, is critical to estimate the anthropogenic aerosols influence on regional climates. Moreover, there are many uncertainties regarding particle effects on the radiative forcing (IPCC 2013).

Brazilian capital cities, which contain millions of inhabitants and vehicles, face many problems concerning air pollution. For most urban areas in Brazil, vehicles are considered the principal source of pollutants emitted to the atmosphere (Andrade et al. 2012).

Vasconcellos (2005) studied the Metropolitan Area of São Paulo (MASP) over years and showed that the economy changed from an industrial profile to that based on services and trades. Now, the MASP is the most important trade region in the country and one of the largest megacities in the world, with more than 20 million inhabitants and 8 million vehicles (Fig. 1). Vehicles are the predominant source of air pollution in São Paulo's Metropolitan Region, but the remote source contribution to local particle concentration is a matter of concern. Some studies have tried to identify other sources: biomass burning (Souza et al. 2014), sea salt aerosol (Andrade et al. 2012), and industrial contribution from the Cubatão city (Gioia et al. 2010), an urban-industrial complex located close to the coast. According to CETESB, the Environmental Agency of São Paulo State, vehicular emissions contribute to 97% of CO emissions, 81% of HC, 78% of NO_x, 43% of SO_x and 40% of PM in MASP (CETESB 2015). The urbanization pattern of the city has resulted in urban heat island effects and rainfall intensity distribution. Rainfall percentages have changed over the recent years; the frequency of severe storms has increased, which might have been influenced by the reduction of green areas, unplanned urbanization, and air pollution, in particular aerosols particles (Siva Dias et al. 2013; Sugahara et al. 2008). Seasonal variation in São Paulo is not so intense. For the winter and summer, the dry and wet seasons, respectively, daily mean temperatures range from 16 °C in July to 28 °C in February. Inhalable particles often exceed the National Ambient Air Quality Standards (NAAQS), mainly during the winter, from June to August (CETESB 2015). Previous studies of particulate matter have been performed in the MASP (Castanho and Artaxo 2001; Miranda et al. 2012; Andrade et al. 2012), demonstrating that aerosol concentrations are higher during the winter and that vehicles emission is the main source of urban pollutants. From August to October, during the biomass burning season in the central region of Brazil and south of the Amazon basin, São Paulo city atmosphere also receives smoke plume pollution transported from those regions (Landulfo et al. 2003; Freitas et al. 2005; Castanho et al. 2008; Landulfo and Lopes 2009; Lopes et al. 2014). During the recent decades, some control policies are being applied and air quality has improved in São Paulo (Carvalho et al. 2015); however, particulate matter and ozone are still exceeding the limits during certain periods of the year.

Urban areas are affected by different combinations of aerosol particles types and spatial and temporal variabilities, inducing different interactions between particles and radiation. As observed in São Paulo, seasonal processes in remote areas, for example, the transport of biomass burning products, can influence the local aerosol optical properties (Zdun et al. 2011; Olcese et al. 2014; Alam et al. 2012). Molnár and Mészáros (2001), while studying concentrations and optical properties of

Fig. 1 Brazil map highlighting São Paulo State and MASP. Red and blue points are University of São Paulo and Meteorological Station, respectively (around 14 km distant from each other). Particulate matter, optical parameters and LIDAR measurements were held on the university campus. Sources: https://en.wikipedia.org/wiki/Water_management_in_the_Metropolitan_Region_of_S%C3%A3o_Paulo#/media/File:SaoPaulo_RR_SaoPaulo.svg and http://www.fflch.usp.br/centrodametropole/562

rural aerosol in Hungary, found that fine particles control scattering and absorption processes and are responsible for 90% of the extinction, pointing out the importance of fine particles to the aerosols climate direct radiative forcing. Zawadzka et al. (2013) used a sunphotometer to measure aerosol optical depth (AOD), a tapered element oscillating microbalance (TEOM) for PM, and moderate resolution imaging spectroradiometer (MODIS) images to characterize aerosols particles properties over different sites in Poland. These areas resemble the MASP, as they are also large urban agglomerations. This study, based on comparison of distinct instruments and methodologies, showed a good relationship between PM concentrations at the surface and AOD. However, the meteorological influence was determinant, considering that some parameters can influence surface measurements of PM but not equally AOD. AOD from a multifilter rotating shadowband radiometer (MFRSR) and Lidar measurements taken in Rome were analyzed over 3 years (2006–2009). The results evidenced the important influence of Sahara dust events on the city aerosol properties, as they modified AOD and Ångström exponent when compared to situations without dust transport (Ciardini et al. 2012).

In the present study, we intended to determine the main chemical characteristics of particles emitted into

the MASP atmosphere during winter (when particle concentrations are higher) and correlate them to their optical properties, taking advantage of simultaneous measurements performed at the surface level, from the orbital platform and vertical distribution data provided by a Lidar system. This methodology was an attempt to use the relationship between information derived using different techniques and instruments in order to analyze the source contributions, local and remote, to the MASP air pollution plume. Satellite observations and ground-based in situ measurements were combined to characterize PM spatial distribution. The latter measurement technique, despite being more accurate, is limited by spatial distribution and, therefore, needs to be used in a complementary way. Surface measurements with samplers allow further physico-chemical characterization of the particles, which combined with particles optical properties retrieved using the MFRSR data can be revealing as regard to the relationship between the MASP aerosol chemical composition and radiative effects. The Lidar system provided the aerosol vertical distribution profiles with high temporal and vertical resolutions. In addition, Hybrid Single-Particle Lagrangian Integrated Trajectory (HYSPLIT) (Draxler and Hess 1998) air mass trajectories were used in synergy with aerosol layers altitude given by the Lidar system to supply information about the sources of the aerosols detected in the MASP atmospheric column during the period analyzed.

Samplings and analysis

In 2012, aerosol sampling at the surface in parallel with particle column integrated optical properties measurements was carried out at the University of São Paulo Campus (USP; 23° 33′ 33.72″ S, 46° 44′ 05.40″ W), which is situated in the western portion of the São Paulo, the main MASP city. The MASP is located 60 km from the Atlantic Ocean and 800 m above sea level. The samplings were carried out during winter (dry season) from August 15 to September 05. Particulate matter was collected using a Partisol-Plus 2025 Sequential Air Sampler and a micro-orifice uniform deposit impactor (MOUDI), which enabled the study of particles concentrations and size distribution. Samples were collected every 12 h with the Partisol and every 24 h with the MOUDI. The rotating MOUDI (Marple et al. 1986) has 10 different stages with varying nominal 50% cutoff (D-50) points: after-filter (0.02), 0.1, 0.18, 0.32, 0.56, 1.0, 1.8, 3.2, 5.6, and 10 μm and inlet (18 μm). The MOUDI worked with 0.4 mm pore diameters, Teflon-backed Nuclepore filters (37 mm after-filter diameter, 1 μm pore size diameter), and a flow rate of approximately 30 L/min. Partisol can sample fine and coarse fractions at the same time. For polycarbonate filters, complementary techniques were employed. Gravimetry was used to determine the total mass through an electronic microbalance with 1 μg readability (MX5; Mettler-Toledo, Columbus, OH, USA). In order to avoid weighting errors, filters were stored in a temperature and humidity-controlled environment (22 ± 2 °C and 45 ± 3% relative humidity) for 24 h prior to their weighting. Blank concentrations were subtracted from the values obtained for each sample. The black carbon concentrations were determined by optical reflectance with a smoke stain reflectometer (model 43D; Diffusion Systems Ltd., London, UK). For this instrument, the calibration curve to convert reflected light to black carbon concentration was obtained empirically using gravimetric standards. The elemental analysis was performed by Energy Dispersive X-ray Fluorescence (EDXRF) to determine the aerosol elemental composition of each sample using an Epsilon 5, PANalytical B.V. instrument. The X-ray tube anode operates with accelerating voltages of 25–100 kV and currents of 0.5–24 mA, with a maximum power of 600 W. The primary target is Sc/W, and the 11 secondary targets (Mg, Al, Si, Ti, Fe, Ge, Zr, Mo, Ag, CaF_2, and CeO_2) can be chosen for measuring different range of elements. A Si(Li) detector with a resolution of 126 eV for Mn Kα was used. Further details are given by Arana et al. (2014). Each filter was submitted to EDXRF, and spectral countings were accumulated for 600 s for elements from Na to K and 300 s for elements from Ca to Pb.

Particles columnar optical properties were retrieved using a MFRSR (Harrison et al. 1994) and vertical profile using a Backscatter Lidar system (MSP-Lidar II). AOD at 415 nm and Ångström exponent (AE; 415 and 670 nm) derived from direct irradiance measurements performed by a calibrated MFRSR following (Rosário et al. 2008) procedures. AE defines the spectral dependence of AOD and depends on the particle size distribution. High AE is associated with fine mode particles dominance and low AE scenarios with coarse mode particles (Seinfeld and Pandis 2006). Ambient scattering coefficient was measured by a Nephelometer 3563-TSI (450 nm), with results presented as 24 h mean data (not until the end of samplings).

The Lidar system consists of a biaxial mode single-wavelength backscatter commercial Raymetrics LR101-

V-D200 system (MSP-Lidar II) that is installed at the Nuclear and Energy Research Institute at USP. Since 2008, it has been part of the Latin American Lidar Network (LALINET), which is a coordinated Lidar network focus on the vertically resolved monitoring of the particle optical properties distribution over Latin America (Guerrero-Rascado et al. 2014, 2016). The light source is a commercial Nd:YAG laser with a fundamental frequency at 1064 nm, which emits pulses of 120 mJ output energy at 532 nm with a repetition rate of 20 Hz and pulse duration of 9.2 ns. The laser beam is vertically directed to the atmosphere, and the backscattered radiation is collected using a Cassegrain telescope with 200 mm diameter, 800 mm focal length, and a 1.25-mrad field of view. The signal acquisition unit consists of a Hamamatsu R9880U-110 PMTs and narrow band interference filters for the elastic backscatter and Raman channel at 532 (0.5) nm and 608 (1) nm, respectively. The PMT output signal is digitized and stored in a Lidar Transient Recorder TR-20-160 (LICEL) with an acquisition analog channel with 12 bits resolution at 20 MHz. Data are averaged with a typical spatial resolution of 15 m and a temporal resolution of 2 min.

The MSP-Lidar II system provides vertical distributions of the aerosol backscatter and extinction coefficients, and also Lidar ratio (LR) values, which is the ratio between extinction and backscattering coefficients. LR values can be assigned to each specific aerosol type (Cattrall et al. 2005; Omar et al. 2005, 2009; Müller et al. 2007). Since there are exclusively daytime

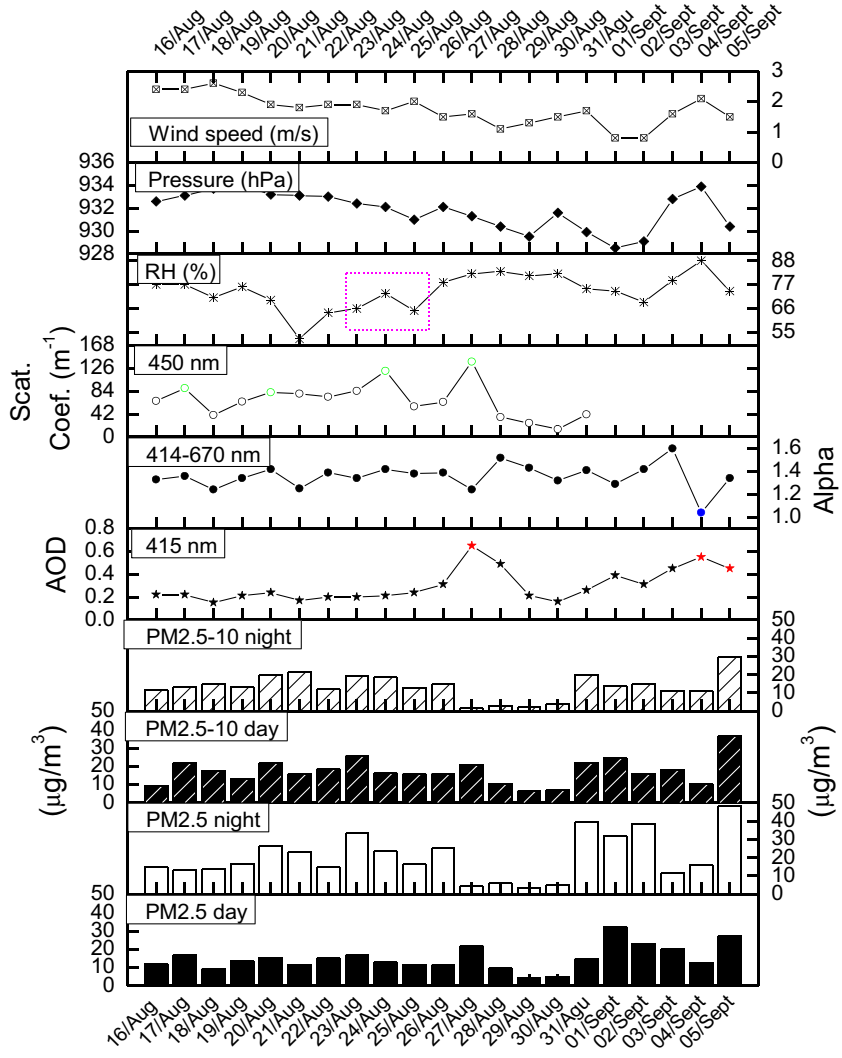

Fig. 2 From *top* to *bottom*: meteorological parameters, aerosol optical properties, and 12-h mean PM concentrations during the sampling period

Table 1 Wind direction predominance and Lidar ratio during the sampling period

Date	Wind predominance	Mean ddaily LR (sr)
Aug. 15	NE	50 ± 10
Aug. 16	NE	
Aug. 17	NE	64 ± 15
Aug. 18	NE	
Aug. 19	NE	
Aug. 20	NE	50 ± 10
Aug. 21	NE	55 ± 11
Aug. 22	NE	63 ± 03
Aug. 23	SE	40 ± 08
Aug. 24	NE	24 ± 07
Aug. 25	NE	
Aug. 26	SE	
Aug. 27	SSE	
Aug. 28	SSE	
Aug. 29	SSE	
Aug. 30	SE	
Aug. 31	SSE	72 ± 15
Sept. 01	C	
Sept. 02	C	
Sept. 03	SSE	75 ± 15
Sept. 04	ESE	
Sept. 05	NE	75 ± 15

measurements during the interested period, only results from the elastic backscatter profiles retrieved applying the Klett-Fernal method analysis will be presented (Fernald et al. 1972; Klett 1981, 1985; Ackermann 1998).

AOD maps from MODIS aboard the Aqua and Terra satellites were used to identify periods of smoke plume transport over São Paulo, since the experiment was conducted during the biomass burning season in central Brazil and southern Amazon basin. Finally, Skew-T log-p diagrams were constructed using the European Centre for Medium-Range Weather Forecasts (ECMWF) ERA Interim daily reanalysis data with 0.75°×0.75° horizontal resolution from 925 up to 200 hPa.

Results

This section is divided in three sub-sections: first, the meteorological conditions during the sampling period are discussed; next, the relationship between aerosol optical properties, meteorological parameters, and elemental composition are presented; and finally, a case study considering the impact of particles from biomass burning on the particles concentration and size distribution at the surface level is performed.

Meteorological conditions

Figure 2 shows the evolution of the meteorological conditions during the sampling period. Meteorological data were provided by the Meteorological Station of the Institute of Astronomy, Geophysics, and Atmospheric Sciences. PM concentrations represent the 12 h mean data and include daytime (7 a.m.–7 p.m. LT) and nighttime (7 p.m.–7 a.m. LT) samples, and the 24 h mean is considered for the other variables. Table 1 presents the dominant wind direction and Lidar ratio (when available).

During the intensive field experiment, mean air temperature, relative humidity, and wind speed were 17 °C, 74%, and 1.7 m/s, respectively. Wind and precipitation are expected to disperse and dilute pollution, thereby lowering PM concentrations. However, there was no significant precipitation registered during the sampling period. Up until August 14, the wind was from the SE, with an average speed of 1.4 m/s. After that day, the wind direction altered and it was decisive for changes in particle composition and optical properties. On August 17, the wind was from the NE with an average speed of 2.5 m/s, which might have contributed to the increase observed in the coarse fraction of aerosol. Winds from the N, NE, and NW can blow urban pollution from other upwind large cities in the state (Campinas, Jundiaí, Vale do Paraíba) to São Paulo, while wind from SE blows air masses from the Atlantic Ocean, which usually changes weather conditions, enhancing the nebulosity.

Increases in the surface particles scattering coefficient were usually related to increases in PM concentrations, which is expected, since both variables were measured at surface level. The observed reduction in particles concentration on August 23–25 and 29–30 was caused by a frontal system passing across the MASP, which decreased air temperature and increased RH and wind speed. Figure 3 presents Skew-T log-p diagrams at 12 UTC for the studied days, showing winds coming from the S and the proximity of the curves T and T_d underscore the high RH (see Fig. 3c, d). A reduction in wind speed on September 1 and 2 resulted in less coarse

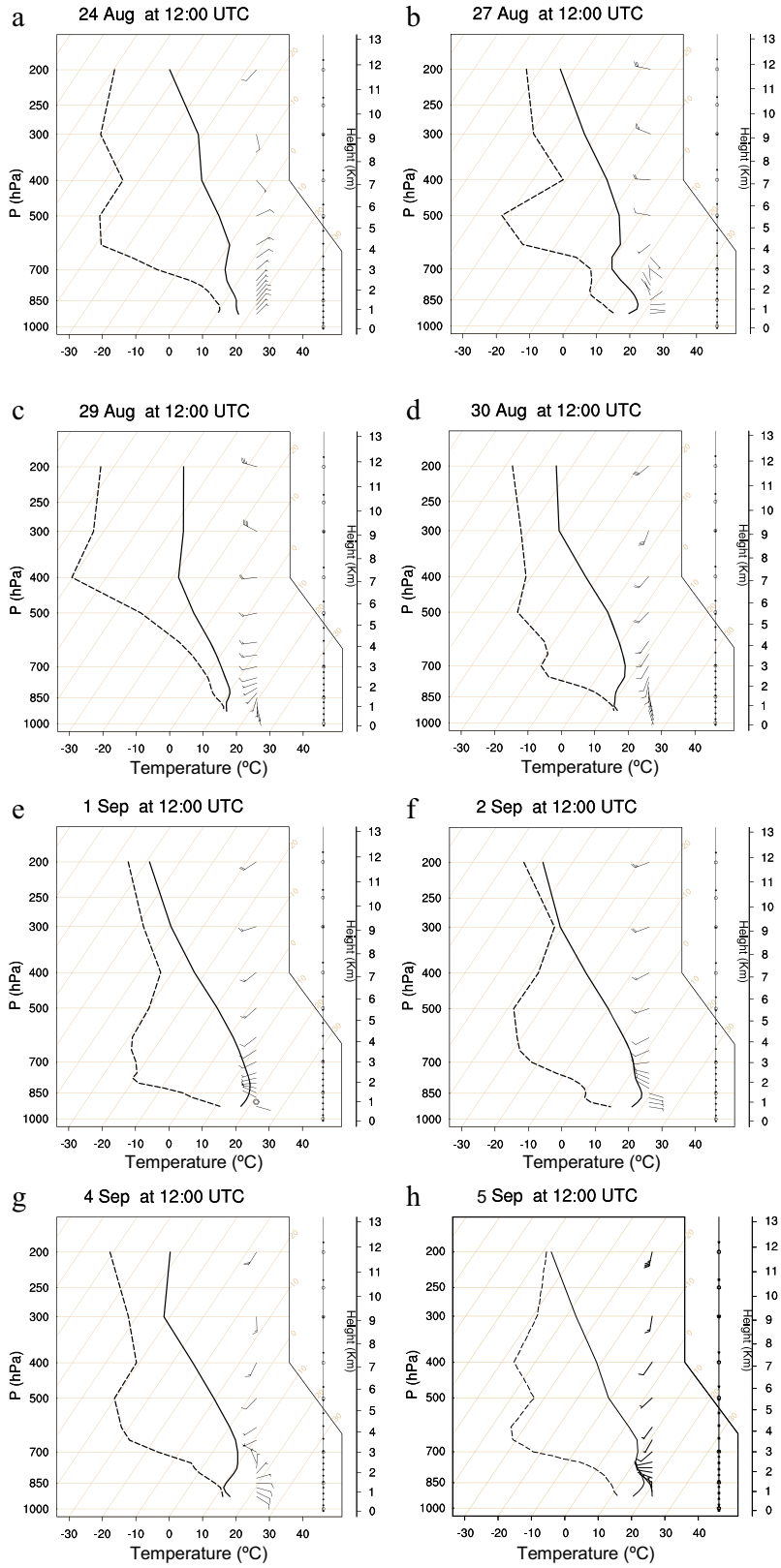

Fig. 3 Skew-T log-p diagrams for selected sampling days. Source: ECMWF at http://apps.ecmwf.int/datasets/data/interim-full-daily

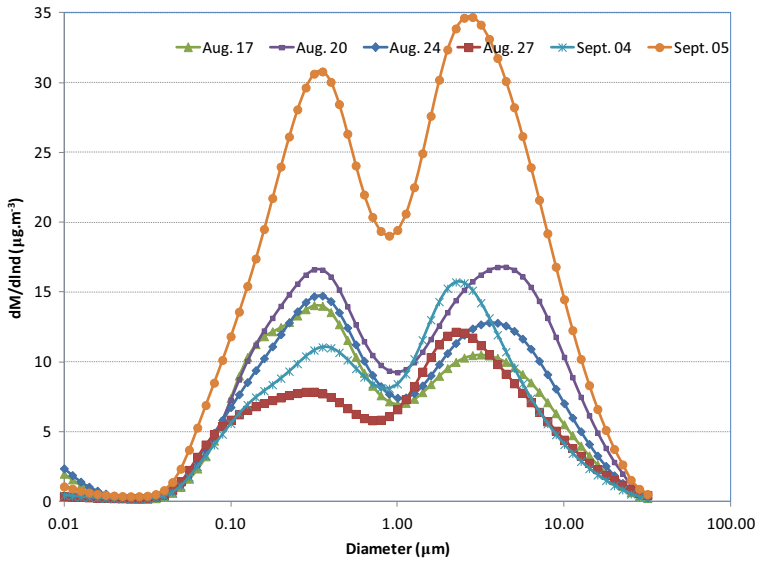

Fig. 4 Mass size distribution based on MOUDI cascade impactor samples

particles in suspension, mainly at night. After the frontal system's passage, which cleaned the atmosphere, the air conditions became stable and unfavorable to dispersion. Thus, changes in wind direction can have a substantial impact on particle concentration, size distribution, and composition. Figure 3e, f shows the temperature profile, wind direction, and T and T_d separation.

Aerosols

According to Fig. 2, the peaks of the scattering coefficient were observed on August 17, 20, 24, and 27 (green circles) when relative humidity was also high, which is possibly due to the effect of scattering by soluble aerosol. Technical problems prevented the nephelometer to work until the end of the experiment. From the data available, it is possible to notice significant increase in AOD from MFRSR measurements on August 27 and September 04 and 05 (red stars). The last period in September was selected for further analysis. In Fig. 4, the particulate matter mass distribution for the selected days, determined based on impactor sample, showed different behaviors.

Intensive optical properties of aerosols are related to their size and elemental composition. Therefore, using the cascade impactor, we performed the X-ray fluorescence analysis for the studied days and the results are shown on Fig. 5. The different scales for black carbon and sulfur are highlighted. As expected, soil elements (Al, Si, Fe, Ca) are more common in the coarser fractions, while S and BC present higher concentrations in the fine fractions.

Mass size distribution illustrates the beginning of particle growth (August, 17), Ångström Exponent starting to decrease. Up until August 20, the coarse fraction increased, along with particle growth. X-ray analysis showed high concentrations for soil elements such as Al, Si, Ca and Fe (Fig. 5). The predominance of coarse particles in the atmosphere contributed to high scattering coefficients until August 20. Samples from the impactor for August 18 were not available, however Partisol data shows higher concentrations in the coarse fraction during the period characterized by low AE.

A low-pressure system that passed rapidly in the region (on 23–25) (dashed pink rectangle in Fig. 2) caused change in wind direction (SE) that brought air masses from cleaner areas of the ocean, which consequently decreased PM concentrations and increased RH and the scattering coefficient. The oceanic winds may have transported particles containing Cl (Fig. 5, August 24), increasing the concentration of hygroscopic particles, which were observed in the enhancement of the scattering coefficient in response to the higher relative humidity. The MSP-Lidar II system retrieved mean LR values of 40 ± 08 sr for August 23, therefore, representing a mixture of local urban aerosol type and possibly sea salt from the ocean, since the typical Lidar ratio values for marine aerosol type range from 20 to 35 sr according to Ansmann et al. (2001) and Franke et al. (2001). As can be seen in Fig. 6 (left panel), the aerosol suspended in the atmosphere was trapped inside

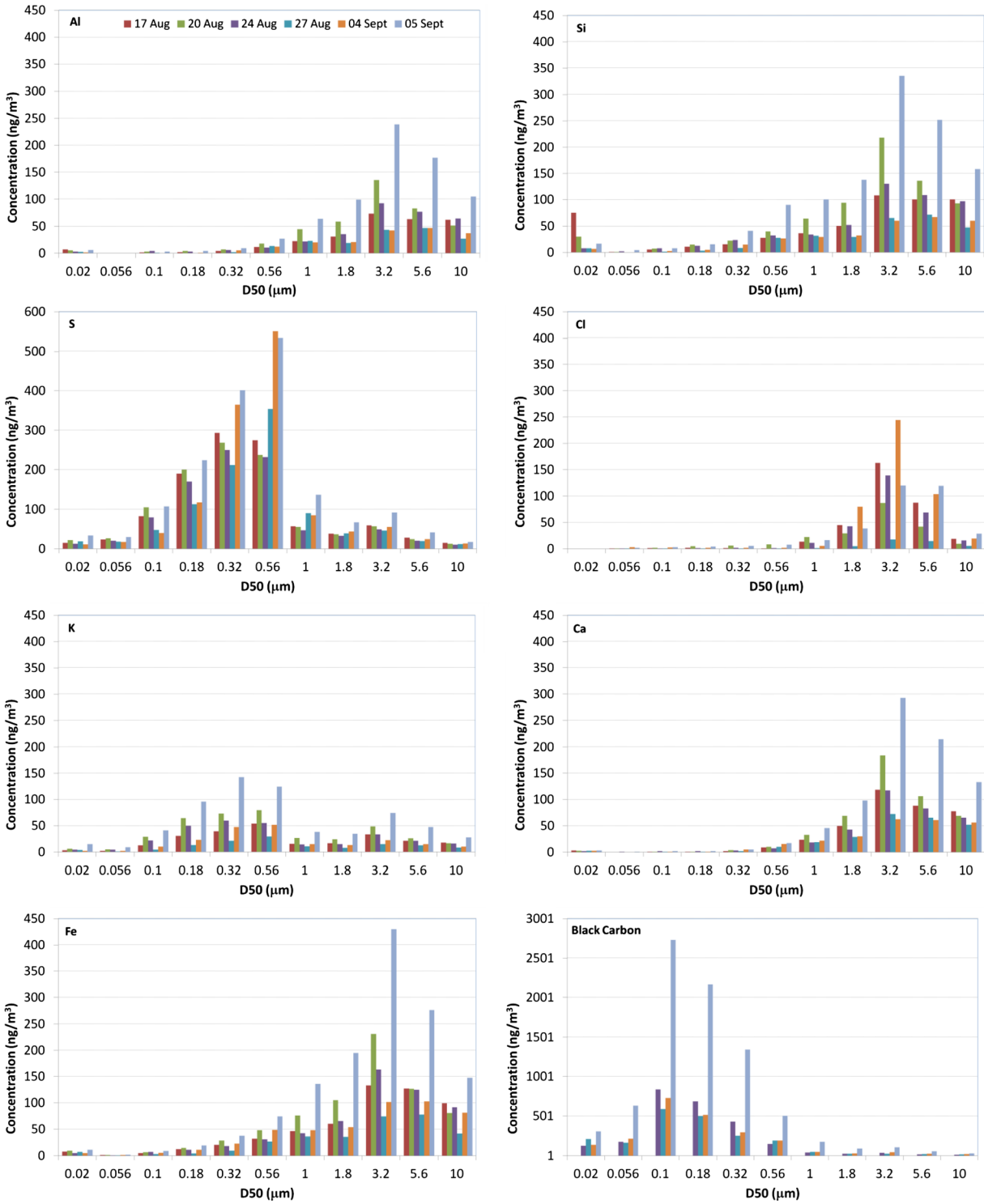

Fig. 5 Temporal variations in mean mass distributions of chemical elements from August 17 to September 05. The different scales for black carbon and sulfur are highlighted

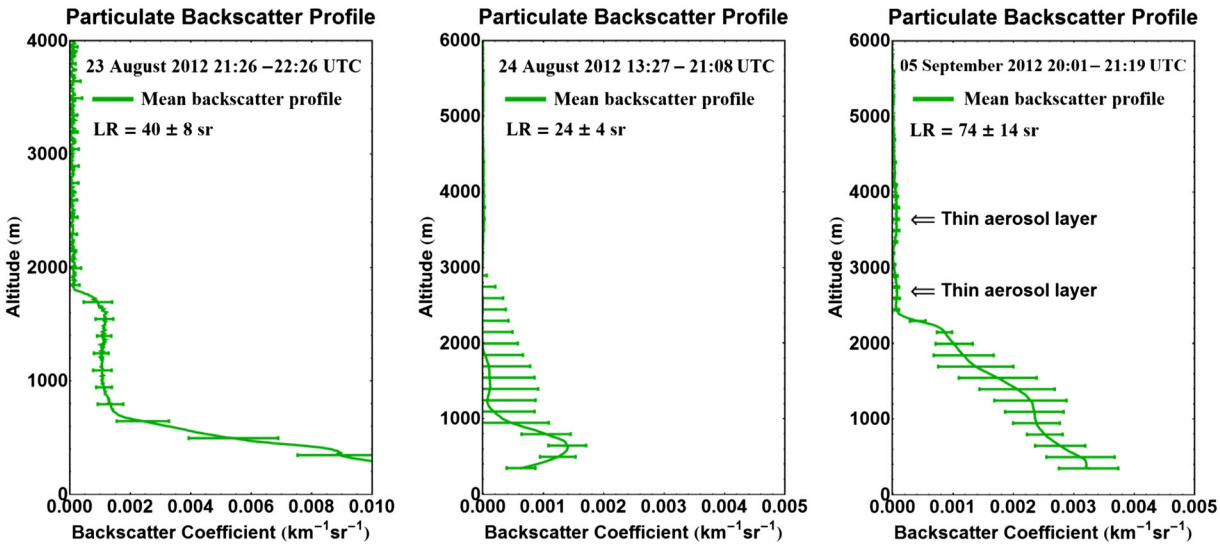

Fig. 6 Vertical profiles of the aerosol backscatter coefficient measured by the MSP-Lidar II system on August 23 and 24 and September 05. The *green line* is the daily mean value of the backscattering coefficient at 532 nm, while the *horizontal bars* represent the standard deviation and indicates the variability of the coefficient during the measurement period

the PBL, under 2000 m of altitude, with no aerosol layers above the PBL. For these measurements, the backscattering coefficient presented a maximum value of 0.010 km^{-1} sr^{-1}, which indicated relatively low quantities of aerosol in the atmosphere (Fig. 6).

Figure 7 shows the air masses backward trajectories computed by the HYSPLIT model that indicated the sources of these aerosol types. Most of the aerosols detected by the Lidar system were transported from the ocean area and could be undergoing a mixture during the process of transportation to the continental area. This fact could justify the Lidar ratio value of 40 sr.

For August 24, we detected very low backscattering coefficient values from the MSP-Lidar II system, with a maximum value of 0.0012 km^{-1} sr^{-1}. This could be related to the oceanic winds carrying particles containing Cl, according to the temporal variations in the mean size distributions of chemical elements presented in Fig. 5 (see also Fig. 2),

The mean LR value retrieved was 24 ± 04 sr, which is a typical Lidar ratio value for marine aerosols, as can be seen in Fig. 6 (middle panel). According to the HYSPLIT air masses backward trajectories, the atmospheric situation remained unchanged from the previous

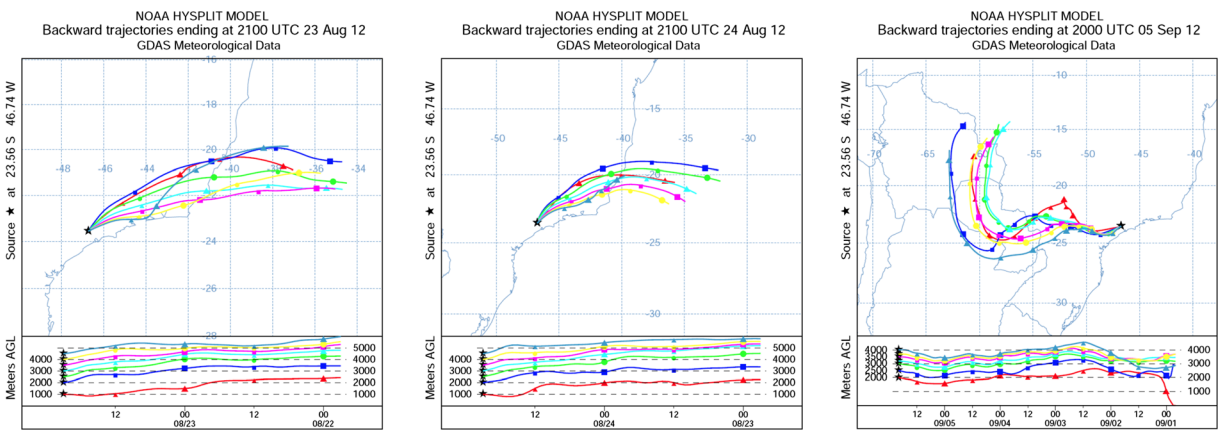

Fig. 7 HYSPLIT backward trajectories ending at the Metropolitan Area of São Paulo on August 23 and 24 at 21 UTC (*left and middle panels*) and on September 5 at 20 UTC (*right panel*)

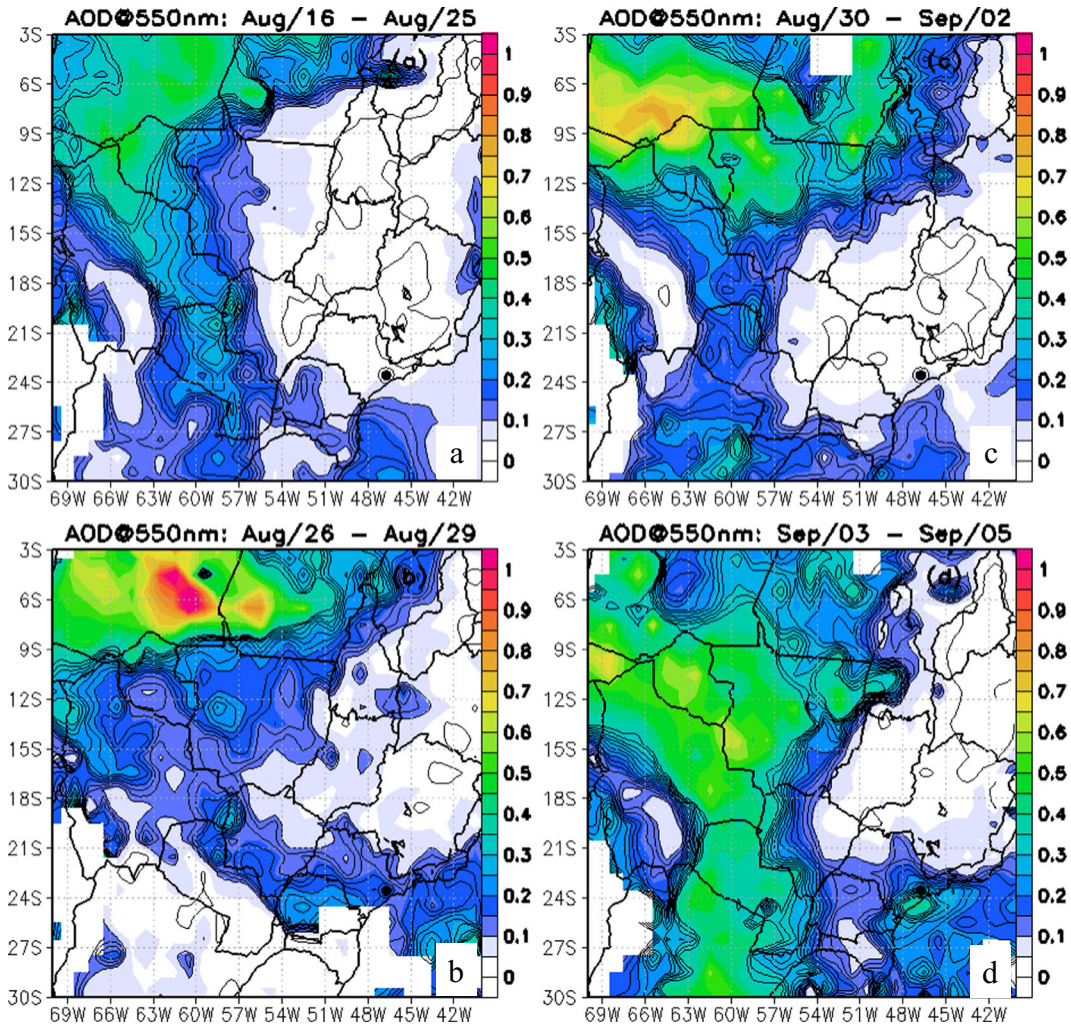

Fig. 8 Aerosol optical depth (AOD) mean field over Brazil from MODIS aboard Aqua satellite considering four scenarios based on AOD variability from ground-based measurements performed at São Paulo city (*black dot*): **a**, **c** Absence of smoke transport over São Paulo. **b**, **d** Smoke transport event over São Paulo

day, with most of the aerosols detected by the Lidar system coming from the ocean area, as presented by the HYSPLIT trajectories shown in Fig. 7 (middle panel). The influence of Cl particles was also observed on September 04, when the wind was blowing from SE after a calm period (Fig. 2).

Both vertical profiles of the aerosol backscattering coefficient presented in Fig. 6 were retrieved using the MSP-Lidar II signal and by applying an inversion method, namely the Klett-Fernald solution for August 23 and September 5. The solution of the lidar equation and the selection of the best lidar ratio value was constrained with AOD from the MFRSR and the MODIS sensor on board the Aqua satellite, following the same procedure described by Marenco et al. (1997) and Landulfo et al. (2003). The error bars were calculated according to the technique described by Guerrero-Rascado et al. (2008).

Further analysis of the AOD enhancement seen by the MFRSR on August 27 and September 5 using AOD fields from MODIS revealed two events of smoke transport from biomass burning regions over São Paulo (Fig. 8). Figure 8a–d shows four scenarios of AOD field over Brazil from MODIS based on AOD variability over the São Paulo from MFRSR. The first scenario consists of MODIS mean AOD field from August 16 to August 25, when São Paulo city was not under the influence of smoke transport. The second scenario, based on mean AOD from August 26 to August 29,

Fig. 9 Map of fire hotspots across Brazil and other countries. Source: INPE—National Institute for Space Research 2016. Portal for the monitoring of vegetation fires. Available at http://www.inpe.br/queimadas. Access on: March 21, 2016

demonstrates that the peak seen by the MFRSR on August 27 over São Paulo was effectively related to a period of smoke transport over the city, which explains the decoupling between the variability of columnar aerosol loading and particles concentration at the surface. The third (from August 30 to September 02) and the fourth (from September 03 to September 05) scenarios represent, respectively, periods when the city was free from smoke transport and again affected by it. During the smoke transport scenarios, Ångström exponent decreased (as can be seen in Figs. 2 and 4) and the scattering coefficient at the surface increased, which suggests an influence of smoke particles at the surface level. Unfortunately, it was not possible to perform Lidar measurements on August 27. However, this subject will be explored during the next section with a case study of biomass burning transportation to MASP on September 05, with high altitude aerosol layers detected by the Lidar system and also HYSPLIT air masses trajectories to determine the sources of aerosols.

Case study: September 05

For September 04, when the lowest Alpha was estimated (blue dot on Alpha data in Fig. 2), the wind speed increased and its direction changed from ESE to NE. On September 05, an AOD peak associated with another smoke transport event was detected by the instruments. Figure 8d shows that the plume related to the AOD peak on September 05 spread all over São Paulo state, with high values of AOD retrieved by the MODIS sensor. The transported plume was responsible for the increased in aerosol concentrations at the surface level and AOD, as well as the lowering of the Ångström exponent (larger particles, Fig. 4). The vertical profile (Fig. 6—right panel) also shows higher values of the backscattering coefficient, mainly in lower altitudes, which can be related to the predominance of soil particles with values of 0.0032 km^{-1} sr^{-1}. The smoke plume contributed to increased concentrations of Al, Si, Ca, Fe, and also S, BC, K, and Cl (Fig. 5) and was detected by the MSP-Lidar II system according to the thin aerosol layers on the vertical backscatter profile (Fig. 6—right panel), at around 2500 to 4000 m high above the surface.

LR values of 50 to 55 sr represent a mixture of dust and urban pollution. Urban pollution presents values between 60 and 75 sr at low altitudes. Values above 70 sr are attributed to biomass burning aerosols in high levels of the atmosphere (Cattrall et al. 2005; Omar et al. 2005; Müller et al. 2007). For September 5, a mean LR value of 75 ± 14 sr was retrieved, with thin aerosol layers detected above the PBL, at altitudes around 2500 to 4000 m, which evidences the presence of biomass burning particles transported from distant areas of

South America, including the central area of Brazil, Paraguay, and Bolivia. Figure 9 shows, for the period, a map of fire points covering a large portion of South America central region.

In addition, the air mass trajectories computed using the HYSPLIT model (Draxler and Hess 1998) helped to identify the origin of the air mass parcels containing smoke aerosol moving toward São Paulo area. Figure 7 (right panel) shows that the 120-h backward trajectories originated in the Central part of South America reached São Paulo at eight different altitudes above ground level. The air masses arriving in São Paulo at the altitudes between 2 and 4 km a.g.l. on September 5 originated from the midwestern region of Brazil and the central region of South America at altitude levels that span from 1 to 3.5 km aboveground level. This is coincident with the period of high AOD, which is mostly due to the smoke advection from biomass burning areas to the São Paulo atmosphere. The arrival altitude of air masses is coincident with aerosol layers, detected by the MSP-Lidar II system on September 5th, in between 2500 to 3000 and 3500 to 4000 m of altitude, as depicted in Fig. 6 (right panel). See also Fig. 3g, h.

Conclusions

In this study, a synergy of different instruments and techniques was employed to investigate the relationship between aerosol microphysical, optical, and chemical properties and other parameters over a sampling period of 15 days in São Paulo city, aiming to identify the impact of local and remote sources of particles.

Despite the shortness of the analyzed period, it was enough to allow us to identify the most relevant aerosol particles sources affecting the MASP atmosphere, from oceanic to biomass burning. The results illustrate that in order to perform a comprehensive assessment of the MASP aerosol particle scenarios, including the identification of minor sources, as biomass burning contribution, it is necessary to consider the synergy of different parameters resulted from multiple techniques of analysis. A cascade impactor and a Partisol particle sampler provided mass concentration and mass size distribution for the aerosol particles. Elemental concentrations were determined by X-ray analysis. Aerosol optical properties, namely optical depth, backscattering coefficients and Ångström exponent, were studied using a multifilter rotating shadowband radiometer and a back-scattering Lidar system. AOD maps from MODIS aboard Aqua satellite were used to identify periods when there were episodes of smoke plume transport over São Paulo. A low pressure system crossing São Paulo caused a decrease of pollutant concentrations, and the consequences on meteorological and aerosol optical parameters were investigated. Higher scattering coefficients were related to periods of high relative humidity. However, one of the maximum concentrations observed during the period coincided with the transport of sea salt, showing enhanced concentration of Cl associated to high relative humidity data. Depending on the wind direction, São Paulo can receive biomass burning from central Brazil and southern regions of the Amazon basin. A case study was performed to further investigate events of smoke transport over São Paulo. Surface instruments and satellite data were analyzed and showed an increase in surface aerosol particles concentrations, with predominance of chemical elements related to biomass burning. The optical parameters were diverse from that found in scenarios dominated by local pollution. The results presented here highlight the complexity of the aerosol mixture observed over MASP and showed that the synergy of different instruments can increase the quality of the study, since aerosol particle information can be evaluated from distinct and yet complementary perspectives.

Acknowledgments This research was supported by the Brazilian agency "Fundação de Amparo à Pesquisa do Estado de São Paulo" (FAPESP; Process number 2008/58104-8, 2011/14365-5, and 2012/24689-5). The authors gratefully acknowledge the NOAA Air Resources Laboratory (ARL) for the provision of the HYSPLIT transport and dispersion model and/or READY website (http://www.ready.noaa.gov) used in this publication. Thanks to the European Centre for Medium-Range Weather Forecasts (ECMWF) for making available the Global Reanalysis ERA Interim data at http://apps.ecmwf.int/datasets/data/interim-full-daily.

References

Ackermann, J. (1998). The extinction-to-backscatter ratio of tropospheric aerosol: a numerical study. *Journal of Atmospheric and Oceanic Technology, 15*, 1043–1050.

Andrade, M. F., Miranda, R. M., Fornaro, A., Kerr, A., Oyama, B., André, P. A., & Saldiva, P. H. (2012). Vehicle emissions and $PM_{2.5}$ mass concentrations in six Brazilian cities. *Air Quality, Atmosphere and Health, 5*, 79.

Ansmann, A. F., Wagner, D., Althausen, D., Müller, D., Herber, A., & Wandinger, U. (2001). European pollution outbreaks during ACE 2: lofted aerosol plumes observed with Raman

lidar at the Portuguese coast. *Journal of Geophysical Research, 106*, 20725–20734.

Alam, K., Trautmann, T., Blaschke, T., & Majid, H. (2012). Aerosol optical and radiative properties during summer and winter seasons over Lahore and Karachi. *Atmospheric Environment, 50*, 234–245.

Arana, A., Loureiro, A. L., Barbosa, H. M., Van Grieken, R., & Artaxo, P. (2014). Optimized energy dispersive X-ray fluorescence analysis of atmospheric aerosols collected at pristine and perturbed Amazon Basin sites. *X-Ray Spectrometry, 43*(4), 228–237.

Carvalho, V. S. B., Freitas, E. D., Martins, L. D., Martins, J. A., Mazzoli, C. R., & Andrade, M. F. (2015). Air quality status and trends over the Metropolitan Area of São Paulo, Brazil as a result of emission control policies. *Environmental Science and Policy, 47*, 68–79.

Castanho, A. D. A., & Artaxo, P. (2001). Wintertime and summertime São Paulo aerosol source apportionment study. *Atmospheric Environment, 35*, 4889–4902.

Castanho, A. D. A., Martins, J. V., & Artaxo, P. (2008). MODIS aerosol optical depth retrievals with high spatial resolution over na urban area using a critical reflectance. *Journal of Geophysical Research, 113*, D0220.

Cattrall, C., Reagan, J., Thome, K., & Dubovik, O. (2005). Variability of aerosol and spectral lidar and backscatter and extinction ratios of key aerosol types derived from selected Aerosol Robotic Network locations. *Journal of Geophysical Research, 110*, D10S11.

CETESB. (2015). São Paulo State Annual Air Quality Report (Relatório de qualidade do ar no Estado de São Paulo), 2014 (in Portuguese—available online at http://ar.cetesb.sp.gov.br/publicacoes-relatorios/). Nov 4, 2015

Ciardini, V., Di Iorio, T., Di Liberto, L., Tirelli, C., Casasanta, G., Di Sarra, A., Fiocco, G., Fuà, D., & Cacciani, M. (2012). Seasonal variability of tropospheric aerosols in Rome. *Atmospheric Research, 118*, 205–214.

Draxler, R. R., & Hess, G. D. (1998). An overview of the HYSPLIT_4 modelling system for trajectories, dispersion, and deposition. *Australian Meteorological Magazine, 47*, 295–308.

Fernald, F. G., Herman, B. M., & Reagan, J. A. (1972). Determination of aerosol height distribution by lidar. *Journal of Applied Meteorology, 11*, 482–489.

Franke, K., Ansmann, A., Müller, D., Althausen, D., Wagner, F., & Scheele, R. (2001). One-year observations of particle lidar ratio over the tropical Indian Ocean with Raman lidar. *Geophysical Research Letters, 28*, 4559–4562.

Freitas, S. R., Longo, K. M., Dias, M. A. F. S., Dias, P. L. S., Chatfield, R., Prins, E., Artaxo, P., Grell, G. A., & Recuero, F. S. (2005). Monitoring the transport of biomass burning emissions in South America. *Environmental Fluid Mechanics, 5*, 135–167.

Guerrero-Rascado, J. L., Ruiz, B., & Alados-Arboledas, L. (2008). Multispectral lidar characterization of the vertical structure of Saharan dust aerosol over southern Spain. *Atmospheric Environment, 42*, 2668–2681.

Guerrero-Rascado, J. L., Landulfo, E., Antuña, J. C., Barbosa, H. M., Barja, B, Bastidas, A. E., Bedoya, A. E., da Costa, R. F., Estevan, R., Forno, R. N., Gouveia, D. A., Jiménez, C., Larroza, E. G., Lopes, F. J. S., Montilla-Rosero, E., Moreira, G. A., Nakaema, W. M., Nisperuza, D., Otero, L., Pallotta, J. V., Papandrea, S., Pawelko, E., Quel, E. J., Ristori P., Rodrigues, P. F., Salvador, J., Sánchez, M. F. & Silva, A. (2014). Towards an instrumental harmonization in the framework of LALINET: dataset of technical specifications, Proc. SPIE 9246, Lidar Technologies, Techniques, and Measurements for Atmospheric Remote Sensing X, 92460O. doi:10.1117/12.2066873.

Guerrero-Rascado, J. L., Landulfo, E., Antuña, J. C., Barbosa, H. M. J., Barja, B., Bastidas, A. E., Bedoya, A. E., Costa, R., Estevan, R., Forno, R. N., Gouveia, D. A., Jimenez, C., Larroza, E. G., Lopes, F. J. S., Montilla-Rosero, E., Moreira, G. A., Nakaema, W. M., Nisperuza, D., Alegria, D., Manera, M., Otero, L., Papandrea, S., Pallota, J. V., Pawelko, E., Quel, E. J., Ristori, P., Rodrigues, P. F., Salvador, J., Sanchez, M., & Silva, A. (2016). Latin American Lidar Network (LALINET): diagnosis on network instrumentation. *Journal of Atmospheric and Solar - Terrestrial Physics, 138–139*, 112–120.

Gioia, S. M. C. L., Babinski, M., Weiss, D. J., & Kerr, A. A. F. S. (2010). Insights into the dynamics and sources of atmospheric lead and particulate matter in São Paulo, Brazil, from high temporal resolution sampling. *Atmospheric Research, 98*, 478–485.

Harrison, L., Michalsky, J., & Berndt, J. (1994). Automated multifilter rotating shadow-band radiometer: an instrument for optical depth and radiation measurements. *Applied Optics, 33*(22), 5118–5125.

INPE 2016. National Institute for Space research. Portal for the monitoring of vegetation fires. Available at http://www.inpe.br/queimadas March 21, 2016.

IPCC (2013). Climate change 2013: the physical science basis. In T. F. Stocker, D. Qin, G.-K. Plattner, M. Tignor, S. K. Allen, J. Boschung, A. Nauels, Y. Xia, V. Bex, & P. M. Midgley (Eds.), *Contribution of Working Group I to the Fifth Assessment Report of the Intergovernmental Panel on Climate Change*. Cambridge: Cambridge University Press 1535 pp.

Klett, J. D. (1981). Stable analytic inversion solution for processing lidar returns. *Applied Optics, 20*, 211–220.

Klett, J. D. (1985). Lidar inversion with variable backscatter/extinction ratios. *Applied Optics, 24*, 1638–1643.

Landulfo, E., Papayannis, A., Artaxo, P., Castanho, A. D. A., de Freitas, A. Z., Ouza, R. F., Vieira Junior, N. D., Jorge, M. P. M. P., Sánchez-Ccoyllo, O. R., & Moreira, D. S. (2003). Synergetic measurements of aerosols over Sao Paulo, Brazil using LIDAR, sunphotometer and satellite data during the dry season. *Atmospheric Chemistry and Physics, 3*, 1523–1539.

Landulfo, E. & Lopes, F. J. S. (2009). Initial approach in biomass burning aerosol transport tracking with CALIPSO and MODIS satellites, sunphotometer, and a backscatter lidar system in Brazil. In: Lidar Technologies, Techniques, and Measurements for Atmospheric Remote Sensing V, 2009, Bellingham. Proceedings of SPIE—Lidar Technologies, Techniques, and Measurements for Atmospheric Remote Sensing V, v. 7479. p. 747905–1–747905-9.

Liu, Y., Jia, R., Dai, T., Xie, Y., & Shi, G. (2014). A review of aerosol optical properties and radiative effects. *Journal of Meteorological Research, 28*, 1003–1028.

Lopes, F.J.S., Moreira, G. A., Rodrigues, P. F., Guerrero-Rascado, J. L., Andrade, M. F., Landulfo, E. (2014). Lidar

measurements of tropospheric aerosol and water vapor profiles during the winter season campaigns over the metropolitan area of São Paulo—Brazil. In: Lidar Technologies, Techniques, and Measurements for Atmospheric Remote Sensing X, 2014, Amsterdam. Proceedings of SPIE - Lidar Technologies, Techniques, and Measurements for Atmospheric Remote Sensing X, 92460H, doi:10.1117/12.2067374.

Marenco, F., Santacesaria, V., Bais, A., Balis, D., di Sarra, D., Papayannis, A., & Zerefos, C. S. (1997). Optical properties of tropospheric aerosols determined by lidar and spectrophotometric measurements (PAUR campaign). *Applied Optics, 36*, 6785–6886.

Marple, V. A., Kenneth, L. R., & Steven, M. B. (1986). A microorifice uniform deposit impactor (MOUDI): description, calibration and use. *Journal of Aerosol Science, 17*, 489.

Miranda, R. M., Andrade, M. F., Fornaro, A., Astolfo, R., André, P. A., & Saldiva, P. H. (2012). Urban air pollution: a representative survey of $PM_{2.5}$ mass concentrations in six Brazilian cities. *Air Quality, Atmosphere and Health, 5*, 63.

Molnár, A., & Mészáros, E. M. (2001). On the relation between the size and chemical composition of aerosol particles and their optical properties. *Atmospheric Environment, 25*, 5053–5058.

Müller, D., Ansmann, A., Mattis, I., Tesche, M., Wandinger, U., Althausen, D., & Pisani, G. (2007). Aerosol-type-dependent lidar ratios observed with Raman lidar. *Journal of Geophysical Research, 112*, D16202.

Olcese, L. E., Palancar, G. G., & Toselli, B. M. (2014). Aerosol optical properties in central Argentina. *Journal of Aerosol Science, 68*, 25–37.

Omar, A. H., Won, J. G., Winker, D. M., Yoon, S. C., Dubovik, O., & McCormick, M. P. (2005). Development of global aerosol models using cluster analysis of Aerosol Robotic Network (AERONET) measurements. *Journal of Geophysical Research, 110*, D10S14.

Omar, A. H., Winker, D. M., Kittaka, C., Vaughan, M. A., Liu, Z., Hu, Y., Trepte, C. R., Rogers, R. R., Ferrare, R. A., Lee, K., Kuehn, R. E., & Hostetler, C. A. (2009). The CALIPSO automated aerosol classification and lidar ratio selection algorithm. *Journal Atmospheric Oceanic Technology, 26*, 1994–2014.

Rosário, N. M. E., Yamasoe, M. A., Sayão, A., & Siqueira, R. (2008). Multifilter rotating shadowband radiometer calibration for spectral aerosol optical depth retrievals over São Paulo City, Brazil. *Applied Optics, 47*, 1171.

Seinfeld, J. H., & Pandis, S. N. (2006). *Atmospheric chemistry and physics: from air pollution to climate change*. New York: Wiley.

Siva Dias, M. A. F., Dias, J., Carvalho, L. M. V., Freitas, E. D., & Silva Dias, P. L. (2013). Changes in extreme daily rainfall for São Paulo, Brazil. *Climatic Change, 116*, 705–722.

Souza, D. Z., Vasconcellos, P. C., Lee, H., Aurela, M., Saarnio, K., Teinila, K., & Hillamo, R. (2014). Composition of $PM_{2.5}$ and PM_{10} collected at urban sites in Brazil. *Aerosol and Air Quality Research, 14*, 168–176.

Sugahara, S., Rocha, R. P., & Silveira, R. (2008). Non-stationary frequency analysis of extreme daily rainfall in São Paulo, Brazil. *International Journal of Climatology, 29*, 1339–1349.

Vasconcellos, E. A. (2005). Urban change, mobility and transport in São Paulo: three decades, three cities. *Transport Policy, 12*, 91–104.

Zawadzka, O., Markowicz, K. M., Pietruczuk, A., Zielinski, T., & Jaroslawski, J. (2013). Impact of urban pollution emitted in Warsaw on aerosol properties. *Atmospheric Environment, 69*, 15–28.

Zdun, A., Rozwadowska, A., & Kratzer, S. (2011). Seasonal variability in the optical properties of Baltic aerosols. *Oceanologia, 53*(1), 7–34.